Published in final edited form as:

J Cell Sci. 2007 October 1; 120(0 19): 3465–3474. doi:10.1242/jcs.005942.

Cdc42 is required for EGF-stimulated protrusion and motility in MTLn3 carcinoma cells

Mirvat El-Sibai[1], **Peri Nalbant**[2,*], **Huan Pang**[1], **Rory J. Flinn**[1], **Corina Sarmiento**[3], **Frank Macaluso**[4], **Michael Cammer**[4], **John S. Condeelis**[3,4], **Klaus M. Hahn**[2], and **Jonathan M. Backer**[1,‡]

[1]Molecular Pharmacology, Albert Einstein College of Medicine, 1300 Morris Park Avenue, Bronx, NY 10461, USA

[2]Pharmacology, University of North Carolina School of Medicine CB7365, Chapel Hill, NC 27599, USA

[3]Anatomy and Structural Biology, Albert Einstein College of Medicine, 1300 Morris Park Avenue, Bronx, NY 10461, USA

[4]Analytical Imaging Facility, Albert Einstein College of Medicine, 1300 Morris Park Avenue, Bronx, NY 10461, USA

Summary

Cdc42 plays a central role in regulating the actin cytoskeleton and maintaining cell polarity. Here, we show that Cdc42 is crucial for epidermal growth factor (EGF)-stimulated protrusion in MTLn3 carcinoma cells. When stimulated with EGF, carcinoma cells showed a rapid increase in activated Cdc42 that is primarily localized to the protruding edge of the cells. siRNA-mediated knockdown of Cdc42 expression caused a decrease in EGF-stimulated protrusion and reduced cell motility in time-lapse studies. These changes were correlated with a decrease in barbed-end formation and Arp2/3 localization at the cell edge, and a marked defect in actin filament branching, as revealed by rotary-shadowing scanning electron microscopy. Upstream of Arp2/3, Cdc42 knockdown inhibited EGF-stimulated activation of PI 3-kinase at early (within 1 minute) but not late (within 3 minutes) time points. Membrane targeting of N-WASP, WAVE2 and IRSp53 were also inhibited. Effects on WAVE2 were not owing to Rac1 inhibition, because WAVE2 recruitment is unaffected by Rac1 knockdown. Our data suggest that Cdc42 activation is crucial for the regulation of actin polymerization in carcinoma cells, and required for both EGF-stimulated protrusion and cell motility independently of effects on Rac.

Keywords

Cdc42; Arp2/3; WAVE2; EGF; Metastasis

‡Author for correspondence (backer@aecom.yu.edu).

*Present address: School of Biosciences, Cardiff University, Museum Avenue, Cardiff, CF10 3US, UK

Supplementary material available online at http://jcs.biologists.org/cgi/content/full/120/19/3465/DC1

Introduction

Cell motility is a fundamental cellular process that is implicated in physiological as well as pathological conditions. The initial steps in cell motility are conserved from *Dictyostelium discoideum* to mammalian cells, and require a biphasic actin-polymerization response leading to membrane protrusion (Chan et al., 1998; Chen et al., 2003; Hall et al., 1989). In carcinoma cells, the actin polymerization transients at 1 and 3 minutes lead to the extension of flat ruffle-free lamellipodia containing a 1-μm-wide zone of F-actin at the leading edge (Segall et al., 1996). Actin nucleation at the leading edge results in the production of a highly branched actin network that provides the protrusive force of the lamellipodia (Bailly et al., 1999; DesMarais et al., 2004; Pollard and Borisy, 2003).

Actin nucleation at the leading edge is dependent on the availability of free barbed ends. Depending on the cell type, these arise from the de novo creation of new filaments, the uncapping of pre-existing filaments, or the severing of F-actin to produce short filaments with free barbed ends (Pollard and Borisy, 2003; Yamaguchi and Condeelis, 2007). In carcinoma cells, cofilin severs pre-existing actin filaments to generate new barbed ends containing ATP-bound actin, to which Arp2/3 preferentially binds (Chan et al., 2000; DesMarais et al., 2004; Ichetovkin et al., 2000; Pollard and Borisy, 2003). Cofilin is inhibited when bound to phosphatidylinositol (4,5)-bisphosphate [PtdIns(4,5)P_2] in the plasma membrane, but is activated by PLCγ-mediated hydrolysis of PtdIns(4,5)P_2, which leads to the release of cofilin from PtdIns(4,5)P_2 in vitro (Matsui et al., 2001; Mouneimne et al., 2004; Yonezawa et al., 1990). This PLCγ/cofilin pathway primarily regulates the early (1 min) barbed end transient and plays an essential role in directional sensing (Mouneimne et al., 2004).

Phosphoinositide 3-kinase (PI3K) is another important regulator of actin polymerization and motility in *D. discoideum*, neutrophils, macrophages, fibroblasts and carcinoma cells (Funamoto et al., 2002; Hill et al., 2000; Huang et al., 2003; Vanhaesebroeck et al., 1999). In both *D. discoideum* and carcinoma cells, the second actin polymerization transient is dependent on the lipid-kinase activity of PI3K and is necessary for membrane protrusion (Chen et al., 2003; Hill et al., 2000; Mouneimne et al., 2004). Recent data from a variety of systems suggest that PI3-kinase activation at the leading edge of moving cells is required for maximal speed of migration but not involved in directional sensing (Andrew and Insall, 2007; Ferguson et al., 2007; Hoeller and Kay, 2007; Nishio et al., 2007). The production of phosphatidylinositol (3,4,5) trisphosphate [PtdIns(3,4,5)P_3] by PI3K activates GTP exchange factors for Rho GTPases, which couples the detection of chemoattractants to actin polymerization (Han et al., 1998; Hawkins et al., 1995; Olson et al., 1996; Ridley, 2001). Rac and Cdc42 can also activate class 1A (p85/p110) PI3K through binding to the BCR domain of p85 (Zheng et al., 1994). In neutrophils, a positive feedback loop between PI3K and Rho GTPases at the leading edge of cells has been proposed (Weiner et al., 2002).

Rac1 and Cdc42 regulate actin polymerization through the activation of WAVE, and WASP and/or N-WASP nucleation factors, which in turn activate the actin Arp2/3 complex (Eden et al., 2002; Rohatgi et al., 1999). The classic initial studies on Rho GTPases used constitutively active and dominant-negative forms of Rho GTPases, and showed that Rac1,

Cdc42 and RhoA regulate the formation of lamellipodia, filopodia and stress fibers, respectively (Nobes and Hall, 1995). In addition to its role in filopodia formation, Cdc42 is important to establish cellular asymmetry during cell motility (Allen et al., 1998; Chou et al., 2003). However, recent advances in single-cell microscopy have documented localized activation of these Rho GTPases that do not fit with their predicted roles. For example, localized Rac activation at the rear of migrating neutrophils (Gardiner et al., 2002), activation of RhoA at the leading edge of growth-factor-stimulated fibroblasts (Kurokawa et al., 2005; Pertz and Hahn, 2004), as well as Cdc42 activation spanning newly formed protrusions in moving fibroblasts (Nalbant et al., 2004), have been observed.

In this study, we describe a major role for Cdc42 in the regulation of protrusion in carcinoma cells. The kinetics of and localization of Cdc42 activation, as well as the effects of Cdc42 knockdown on actin nucleating proteins and barbed end formation, suggest a critical role for this Rho GTPase in actin polymerization and lamellipod formation. Our data show that in MTLn3 carcinoma cells, Cdc42 directly regulates lamellipod extension in a Rac-independent manner.

Results

Spatial and temporal analysis of Cdc42 activation in EGF-stimulated carcinoma cells

In response to EGF stimulation, MTLn3 carcinoma cells rapidly extend a thin, flat ruffle-free lamellipod, which is maximal at 3–5 minute and contains a zone of F-actin at the protruding edge (Rotsch et al., 2001; Segall et al., 1996). In order to examine the role of Cdc42 in these processes, we studied the kinetics and distribution of Cdc42 activation in MTLn3 cells. Using a GST-CRIB pull-down assay, we found that total cellular Cdc42 was maximally activated after 1 minute of EGF stimulation, and returned to close to basal levels by 4 minutes (Fig. 1A). Cdc42 activation was abolished in wortmannin-treated cells (Fig. 1B), consistent with the requirement for PI 3-kinase during EGF-stimulated protrusion (Hill et al., 2000). Immunostaining with anti-Cdc42 antibody showed that Cdc42 localized to the protruding edge in response to EGF stimulation (Fig. 1C). The staining was specific because it was abolished by pre-incubation of the anti-Cdc42 antibody with recombinant GST-Cdc42 (supplementary material Fig. S1A) or by knockdown of Cdc42 by using small interfering RNA (siRNA) (supplementary material Fig. S1B). The kinetics of Cdc42 accumulation in the actin nucleation zone (0.6 μm in from the cell periphery) was similar to that seen in total cell lysates (Fig. 1D). The presence of Cdc42 in the region of new actin polymerization was confirmed in cells co-stained with Rhodamine-phalloidin (supplementary material Fig. S1C), where the merged images show localization of Cdc42 to the F-actin-rich protruding edge.

Changes in the localization of small GTPases do not directly measure their activation. We therefore used a recently developed Cdc42 biosensor that detects endogenous activated Cdc42 in single cells (Nalbant et al., 2004). The biosensor contains GFP linked to a merocyanine-dye-labeled CRIB domain, designed so that ratio of dye to GFP fluorescence increases with Cdc42 binding. Normalization of dye-fluorescence output to GFP also corrects for variations in cell thickness, probe distribution and field illumination (Nalbant et al., 2004). Control experiments demonstrated normal EGF-stimulated cytoskeletal responses

in cells that were microinjected with the biosensor (data not shown). We examined Cdc42 activation in fixed MTLn3 cells (n=40 cells per time point). After EGF stimulation, Cdc42 showed acute activation in a narrow area at the edge of actively protruding lamellipods (Fig. 1E). In contrast to the data in Fig. 1A and B, which show Cdc42 activation in the whole cell and Cdc42 localization to the leading edge, respectively, Cdc42 activation at the cell edge was biphasic, with peaks of activation at 50 seconds and 3 minutes after EGF stimulation (Fig. 1F). No activation was seen with a mutant construct that cannot bind Cdc42 (Fig. 1E, upper left panel). Thus, Cdc42 activation kinetics at the protruding edge coincided with the kinetics of barbed-end formation in MTLn3 cells, which also shows transients at 1 and 3 minutes (Chan et al., 1998).

Cdc42 is required for maximal protrusion in EGF-stimulated carcinoma cells

The similar kinetics of Cdc42 activation and actin polymerization in EGF-stimulated carcinoma cells suggested a direct role for Cdc42 in actin nucleation and lamellipod extension. To test this hypothesis, we knocked down expression of Cdc42 with siRNA. Cdc42 expression was reduced by 80% as compared with cells transfected with control siRNA duplexes (Fig. 2A). EGF-stimulated protrusion in Cdc42 siRNA-treated cells was significantly decreased as compared with control-siRNA-treated cells (Fig. 2B, C). As opposed to the flat, thin, phase-dense lamellipodia seen at the edges of control cells, the protrusions in Cdc42 siRNA-treated cells appeared to be thicker and to lack a well-defined phase-dense cell edge (Fig. 2B). Kymographic analysis of cells protruding in serum furthermore revealed the lack of persistent protrusions in the Cdc42 siRNA-treated cells (Fig. 2D). Unlike control cells, where the cell edge protruded a mean distance of 4.0±1.0 μm beyond the focal adhesions (supplementary material Fig. S3A, B), in EGF-stimulated Cdc42-knockdown cells the cell edge protruded only 1.8 ±0.1 μm beyond the focal adhesions. Consistent with the effect on cell protrusion, knockdown of Cdc42 also led to an approximate twofold decrease in steady-state cell motility in serum (Table 1; see supplementary material Movies S1, S2 and Fig. S3C). Knockdown of Cdc42 with a distinct pool of siRNA oligonucleotides produced similar effects on protrusion and motility (supplementary material Fig. S4A, B; see also Table 1). The effects of Cdc42 knockdown were not owing to secondary effects on EGF receptor signaling, because activation of Erk1/2 and EGF-stimulated receptor internalization were minimally affected by Cdc42 knockdown (supplementary material Fig. S4C, D). Knockdown of Cdc42 also inhibited insulin-stimulated protrusion (supplementary material Fig. S4E).

Cdc42 plays a role in actin polymerization, barbed-end formation and Arp2/3-dependent actin branching

The inhibition of EGF-stimulated protrusion in Cdc42 siRNA-treated cells coincided with a marked reduction in F-actin accumulation at the edge of protruding cells (Fig. 3A, B). To identify the mechanism for this reduced protrusive activity and actin polymerization, we measured the formation of new barbed ends in EGF-stimulated MTLn3 cells. Cdc42 knockdown led to a partial decrease in barbed end formation after 1 minute of EGF stimulation, but a near complete inhibition of barbed end formation at 3 minutes (Fig. 3C, D). Consistent with this, the recruitment of the Arp2/3 complex to the protruding edge,

another crucial step in actin-mediated protrusion (Bailly et al., 2001; Bailly et al., 1999), was significantly reduced by Cdc42 knockdown (Fig. 4A, B).

The protruding edge, where new barbed ends are formed, is rich in F-actin and actin-nucleating factors such as Arp2/3, but contains little tropomyosin. Tropomyosin staining is only seen at distances greater than 1 μm behind the edge of the lamellipod, and defines the tropomyosin-rich lamellar region (DesMarais et al., 2002; Ponti et al., 2004). In agreement with these reports, we found that tropomyosin was largely excluded from the zone of actin polymerization defined by Arp2/3 in control cells (Fig. 4A, left panel and 4C, top panel). By contrast, tropomyosin staining in Cdc42-knockdown cells extended to the extreme edge of these cells (Fig. 4A, right panel and 4C, lower panel). Thus, in cells in which Cdc42 expression is suppressed, EGF-stimulated protrusion does not extend beyond the lamellar region, and the actin-rich lamellipodial compartment does not form.

The absence of Arp2/3 at the cell edge would be expected to cause a significant derangement of F-actin structure due to the loss of Arp2/3-mediated branching. We examined actin structure at high resolution in control and Cdc42-siRNA-treated cells using rotary-shadowing electron microscopy. Control cells showed a highly branched actin network – the average incidence angle was 38.2° ±1.6, as defined in Bailly et al. (Bailly et al., 1999) and DesMarais et al. (DesMarais et al., 2004), typical of a lamellipods in MTLn3 cells (Fig. 5, left panel). The Cdc42-knockdown cells showed a marked defect in actin branching, which led to an irregular actin network with an increase in incidence angle (46° ±1.8) consistent with inhibition of Arp2/3 complex activity (DesMarais et al., 2004), and longer actin filaments that are more typical of the lamellar region (Fig. 5, right panel). Thus, in Cdc42-knockdown cells, long unbranched filaments frequently reach the edge of the cell, whereas, in control cells, long filaments remain behind the actin nucleation zone, leaving branched shorter filaments at the edge (Fig. 5).

Cdc42 is required for the translocation of N-WASP and WAVE2 to the protruding edge

Activation of Arp2/3-mediated branching involves its interactions with actin-nucleation factors, such as N-WASP and WAVE2, the predominant WASP-family members in MTLn3 cells (C.S. and J.C., unpublished). Cdc42 regulation of N-WASP has been well described, and N-WASP membrane translocation in EGF-stimulated cells was markedly attenuated by Cdc42 knockdown (Fig. 6A, B). Similarly, EGF-stimulated recruitment of WAVE2 to the lamellipod was readily detected in control-siRNA-treated cells, but was abolished in Cdc42-siRNA-treated cells (Fig. 6C, D).

Whereas Cdc42 interacts directly with N-WASP (Miki et al., 1998), its regulation of WAVE2 is likely to involve intermediary proteins. Potential mechanisms of Cdc42 activation of WAVE2 include (1) activation of Class IA PI 3-kinase though Cdc42 binding to the p85 BCR domain (Zheng et al., 1994), leading to increases in PtdIns(3,4,5)P_3 that can recruit WAVE2 via a basic domain in the WAVE2 N-terminus (Oikawa et al., 2004) and, (2) activation of Rac (Hall, 1998), which binds to WAVE2 via the IRSp53 adapter (Miki et al., 2000); however, is also conceivable that, (3) a CDC42-IRSp53 complex could directly interact with WAVE2 (Krugmann et al., 2001), although this has not been demonstrated and

Cdc42/IRSp53/WAVE2 binding was not detected in EGF-stimulated A431 cells (Suetsugu et al., 2006).

We tested the effect of Cdc42 knockdown on upstream regulators of WAVE2 in MTLn3 cells. We found that Rac and Cdc42 colocalized in the protruding edge of control MTLn3 cells after EGF stimulation (supplementary material Fig. S5A). Furthermore, Rac localization to the protruding edge (Fig. 7A) and loading of Rac-GTP (supplementary material Fig. S5B) was inhibited by Cdc42 knockdown. PtdIns(3,4,5)P_3 accumulation at the protruding edge of EGF-stimulated MTLn3 cells was also markedly inhibited in Cdc42-knockdown cells (Fig. 7B), as was EGF stimulation of Akt (supplementary material Fig. S5C). Finally, EGF-stimulated translocation of IRSp53 to the protruding edge is clearly visible in control cells but is significantly reduced in Cdc42-siRNA-treated cells (Fig. 7C). Taken together, these data show that the three potential mechanisms for activation of WAVE2 in EGF-stimulated cells are all inhibited when Cdc42 is depleted.

The inhibition of WAVE2 recruitment to the protruding edge in Cdc42-knockdown cells could be a secondary effect owing to inhibition of Rac1. However, we find that WAVE2 recruitment to the protruding edge is unaffected by knockdown of Rac1 in MTLn3 cells (supplementary material Fig. S5D). Taken together with our previous finding that Rac1 knockdown does not affect protrusion in MTLn3 cells (Yip et al., 2007), our data suggest that the effects of Cdc42 knockdown on WAVE2 are independent of Rac.

Independent roles for Ras and Cdc42 in PtdIns(3,4,5)P_3 production and protrusion

We have recently shown that EGF stimulation of K-Ras is required for activation of PI 3-kinase at late time (after 3–4 minutes of EGF stimulation), and is important EGF-stimulated for protrusion (Yip et al., 2007). The differential effects of Cdc42 knockdown versus K-Ras knockdown on PtdIns(3,4,5)P_3 production, with inhibition at 1 minute versus 3 minutes, respectively, suggests that the two GTPases act in a mechanistically independent manner. To test this, we measured the activation of Ras and Cdc42 after knockdown of each GTPase. As expected, knockdown of Cdc42 had no effect on Ras activation (supplementary material Fig. S6A), and knockdown of K-Ras had no effect on Cdc42 activation (supplementary material Fig. S6B).

Discussion

Current models suggest that actin polymerization at the protruding edge of a moving cell involves the local activation of Rac, which engages the WAVE members of the N-WASP family through a complex of proteins including IRSp53, Abi1, Nap1 and PIR121, leading to Arp2/3-mediated actin filament nucleation and branching (Soderling and Scott, 2006; Stradal and Scita, 2006). The precise roles of these Arp2/3 regulatory proteins are still controversial (Innocenti et al., 2004; Oikawa et al., 2004). Nonetheless, the result of this localized actin polymerization is the application of protrusive force to the cell membrane, and the extension of a lamellipod.

By contrast, the work described here and by Yip et al. (Yip et al., 2007) suggest a different model for the roles of small GTPases during protrusion. As we have recently shown,

siRNA-mediated knockdown of Rac1, the major isoform expressed in MTLn3 carcinoma cells, has little effect on EGF-stimulated protrusion (Yip et al., 2007). By contrast, knockdown of Cdc42 has pleiotropic inhibitory effects on cytoskeletal signaling, with suppression of PtdIns(3,4,5)P_3 generation at early times after stimulation (1 minute), Rac activation, N-WASP, WAVE2 and IRSp53 recruitment, and Arp2/3-mediating branching. These changes result in reduced protrusion in response to EGF, and reduced motility. Ras signaling is also required for protrusion, because knockdown of K-Ras blocks PtdIns(3,4,5)P_3 production at late times after EGF stimulation (3 minutes) and also inhibits protrusion (Yip et al., 2007). The K-Ras and Cdc42 pathways appear to be distinct, as knockdown of Cdc42 does not affect Ras activation and vice versa.

Parallel studies in MTLn3 carcinoma cells on the roles of Rac and Ras (Yip et al., 2007), Cdc42 (this paper), Arp2/3 (DesMarais et al., 2004), and cofilin (Chan et al., 2000; DesMarais et al., 2004) make it possible to propose a model for EGF signaling to the cytoskeleton in carcinoma cells (Fig. 8). Acute EGF stimulation of quiescent cells leads to the rapid activation of PLCγ, Ras, Rac, Cdc42 and class IA PI 3-kinase, all of which reach maximal levels of activity within 1 minute (Mouneimne et al., 2004; Yip et al., 2007) (this paper), coincident with the first peak of actin polymerization (Chan et al., 1998). PLCγ is presumably activated by SH2-mediated recruitment to the EGFR and subsequent tyrosine phosphorylation (Chattopadhyay et al., 1999), whereas Ras is likely to be activated by binding of Grb2-SOS complexes to the EGFR or to tyrosine-phosphorylated Shc (Schlessinger, 1993). The PI 3-kinase activity peak at 1 minute requires a positive feedback loop with Cdc42, because PtdIns(3,4,5)P_3 production at 1 minute is diminished in Cdc42-knockdown cells and Cdc42 activation is blocked by PI 3-kinase inhibitors. PI 3-kinase activity is also augmented by inputs from Ras, albeit at somewhat later times (3–4 minutes) (Yip et al., 2007).

Activation of Cdc42 and PLCγ both contribute to barbed-end formation during the first actin transient (this paper) (Mouneimne et al., 2004). PLCγ hydrolysis of membrane PtdIns(4,5)P_2 leads to cofilin activation and early (1 minute) barbed-end production. Subsequent barbed end formation by cofilin-mediated severing is sufficient for directional sensing and is significantly reduced by inhibition of the PLCγ-cofilin pathway (Mouneimne et al., 2006; Mouneimne et al., 2004). The Cdc42 pathway may contribute to PLC activation, as Cdc42 binds directly to PLCγ in RBL-2H3 cells and in EGF-stimulated fibroblasts (Chou et al., 2003; Hong-Geller and Cerione, 2000).

By contrast, the later actin transient (at 3 minutes) is dependent on PI 3-kinase, whose activation at late times requires K-Ras (Yip et al., 2007). Barbed-end production at late times is thought to be involved in the production of mechanical force during protrusion (Mouneimne et al., 2004). Interestingly, although both K-Ras and PI 3-kinase activity are necessary for the late actin transient (Yip et al., 2007), they are not sufficient to generate it, because knockdown of Cdc42 leads to an inhibition of barbed ends at 3 minutes but does not affect Ras activation or PtdIns(3,4,5)P_3 production at 3 minutes. Thus, the delay or a decrease in lamellipod extension caused respectively by inhibition of PLCγ or Cdc42 (Mouneimne et al., 2004) (this paper) may reflect a requirement for the first actin in the generation of the second.

Downstream of Cdc42, both N-WASP and WAVE2 are activated and recruited to the plasma membrane. The effects of Cdc42 knockdown on WAVE2 do not appear to be due to decreased Rac1 activation; we find that because WAVE2 recruitment is normal in EGF-stimulated Rac1-knockdown cells. Whereas the Cdc42-dependent links to WAVE2 in MTLn3 cells have not been clearly established, knockdown of Cdc42 inhibits PtdIns(3,4,5)P_3 production and recruitment of IRSp53 to the membrane, processes that have both been implicated in WAVE2 activation in various systems (Miki et al., 2000; Oikawa et al., 2004). The effects of Cdc42 knockdown on both N-WASP and WAVE2 lead to a decreased activation of Arp2/3, and decreased actin branching at the protruding edge of the cells. Finally, Cdc42-mediated activation of Rac may also enhance motility through the formation of focal complexes at the leading edge, because focal complex formation is inhibited by Rac1 knockdown (Yip et al., 2007).

Our work is consistent with a number of previously described systems in which the canonical roles of Rho, Rac and Cdc42 do not hold. For example, macrophages that lack all Rac isoforms show migration speeds similar to that of wild-type macrophages and are capable of chemotaxis towards CSF1 (Wheeler et al., 2006). Although membrane ruffling is reduced, these cells can extend protrusions that result in cell motility. Similarly, RAW 264.7 cells, transfected with dominant-negative constructs for Cdc42 but not Rac1, inhibit PMA-induced ruffling (Cox et al., 1997), and membrane ruffling and lamellipod formation in clone A colon carcinoma cells are inhibited by dominant-negative constructs for RhoA but not Rac1 (O'Connor et al., 2000).

Why do MTLn3 cells rely on Cdc42 rather than Rac for generation of protrusions? A potential answer lies in the fact that MTLn3 cells have elevated levels of activated Rho as compared with their non-metastatic MTN progenitor (M.E.-S., unpublished). Recent data suggest that inhibition of Rho in MTLn3 cells leads to activation of Rac but not Cdc42 (M.E.-S., unpublished), suggesting that Rac signaling is relatively suppressed in these cells. In the face of this Rho-mediated Rac suppression, Cdc42 may play a compensatory role in protrusion. This hypothesis suggests that the reliance on Rac versus Cdc42 for protrusive activity will vary in different cell types, depending on the relative activity of the Rho-ROCK pathway. Thus, the clinical consequence of targeting the upstream activators of Rac versus Cdc42 might depend on the status of Rho signaling pathways in a given tumor.

Materials and Methods

Cell culture

Rat mammary adenocarcinoma cells, MTLn3 cells, were cultured in α-MEM medium supplemented with 5% FBS. For experiments, cells were starved in L15 media (GIBCO BRL) with 0.35% BSA for 3 hours, and stimulated with a final concentration of 5 nM murine EGF for various times (Upstate Biotechnology, Lake Placid, NY). For microscopy, cells were plated on coverslips coated with rat-tail type 1 collagen (BD Biosciences, Bedford, MA) or on collagen-coated dishes (MatTek Corporation) 24 hours prior to the experiment.

Antibodies and reagents

Rabbit polyclonal anti-Cdc42 antibody (sc-87) and goat polyclonal anti-WAVE2 antibody (C-14) were obtained from Santa Cruz Biotechnology. Mouse monoclonal anti-Rac (clone 23A8), mouse monoclonal anti-paxillin (clone 5H11), mouse monoclonal anti-cortactin (p80/p85) (clone 4F11) and rabbit polyclonal anti-Arp3 antibodies were purchased from Upstate Biotechnology. Mouse monoclonal anti-tropomyosin (TM311) has been previously described (DesMarais et al., 2002). Mouse monoclonal anti-PtdIns(3,4,5)P_3 IgG was obtained from Echelon Biosciences Incorporated. Mouse monoclonal anti-phospho-tyrosine antibody (*P*-Tyr-100), rabbit polyclonal anti-*P*-ERK1/2 (Thr202/Tyr204), mouse monoclonal anti-(Ser473)-Akt and rabbit polyclonal anti-Akt antibodies were obtained from Cell Signaling Technology. The goat polyclonal anti-IRSp53 antibody was obtained from Abcam Inc. Anti-Ras antibody (Y13-259) was provided by T. Michaeli (AECOM, New York, NY). Cy5-conjugated anti-biotin was obtained from Jackson ImmunoResearch Laboratories. Rhodamine-phalloidin, Cy5-palloidin and fluorescent secondary antibodies were obtained from Molecular Probes. GFP-vinculin was a generous gift from Stefan Huettelmaier, AECOM, New York, NY.

Protein purification

GST fusion proteins containing the PAK1 GTPase-binding domain (hPAK(67-150), CRIB domain), or the Raf1 Ras-binding domain (aa 51-131, RBD domain) (generous gift from Linda van Aelst, Cold Spring Harbor Laboratory, NY) were purified from *Escherichia coli*. The proteins were purified by binding to glutathione-Sepharose (Amersham Biosciences). The purity and concentration of the proteins was determined by SDS-PAGE and Coomassie-Blue staining.

Pull-down assays

MTLn3 cells were starved for 3 hours, stimulated with EGF for various times and stopped by the addition of ice-cold PBS containing with 1 mM sodium orthovanadate. The cells were lysed and incubated with GST-CRIB or GST-RBD and the pull-down assay performed as previously described (Benard and Bokoch, 2002). GTP-Cdc42, GTP-Rac or GTP-Ras were detected by western blotting using the anti-Cdc42, anti-Rac or anti-Ras antibodies. Quantification was done by densitometry using the NIH image 1.62 analysis software.

Immunostaining

After EGF stimulation, cells were saponin-permeabilized and fixed as previously described (Eddy et al., 2000) for 30 minutes at 37°C. Cells were then rinsed with PBS, and aldehyde autofluorescence was quenched with 1 mg/ml $NaBH_4$. For blocking, cells were incubated with 1% BSA, 1% FBS in PBS for 30 minutes. Cells were stained with primary antibodies for 2 hours and with secondary antibodies for 2 hours. For the barbed-end assay, cells were permeabilized with saponin and incubated with biotin-labeled G-actin (Cytoskeleton, Inc.), then stained with anti-biotin as described (Chan et al., 1998). For the pre-absorption experiment, cells were stained with anti-Cdc42 antibody pre-incubated in solution with GST alone or with GST-Cdc42 for 1 hour at 4°C prior to staining. All fluorescent images were taken using a 60× 1.4 NA infinity-corrected optics on a Nikon Eclipse microscope

supplemented with a computer-driven Roper cooled CCD camera and operated by IPLab Spectrum software (VayTek). We have previously shown, using atomic-force microscopy, that the height of the lamellipod in EGF-stimulated MTLn3 cells is approximately 600–800 nm (Rotsch et al., 2001). Thus, the entire lamellipod is within one optical section and the use of confocal microscopy was not necessary. For image analysis, all digital images were imported in image J software (National Institutes of Health, MA). For quantification of the mean fluorescent intensity at the cell edge, images were analyzed using a previously described macro (DesMarais et al., 2002). For quantification of adhesion structures, a line was drawn from the cell edge to each focal adhesion cluster and the distance measured in image J software.

Purification and labeling of recombinant eGFP-CBD-ISO-IAA proteins

The wild-type eGFP-tagged Cdc42-binding fragment of human WASP (eGFP-CBD) construct as well as that carrying a mutation in the Cdc42-binding site (H246D, H249D) were obtained from Klaus Hahn (Nalbant et al., 2004). The proteins were expressed and purified using the Qiagen expressionist kit according to the manufacturer's instructions. The concentration of the protein was quantified using absorbance at 280 nm (CBD, ε =8250 cm^{-1} M^{-1}). The labeling was performed as previously described (Nalbant et al., 2004). The purified proteins were dialyzed against 50 mM sodium phosphate (pH 7.5) and labeled with fluorescent dye ISO-IAA (Toutchkine et al., 2003) at a 6:1 ratio of dye to protein, at room temperature for 90 minutes. The conjugates were then desalted using desalting spin columns (Pierce). The labeling efficiency was 90%. Concentrationof the eGFP-CBD-ISO-IAA conjugate was calculated using the eGFP absorbance at 488 nm (eGFP, ε=61000 cm^{-1} M^{-1}).

EGFP-CBD-ISO-IAA image acquisition and analysis

Cells plated on coverslips were starved for 12 hours in serum-free medium and then microinjected with 50 μM dye-labeled eGFP-CBD using an Eppendorf 5171/5242 semi-automatic micromanipulator/microinjector. The cells were allowed to recover for 1 hour before stimulation, fixation and imaging. The fluorescent filters used have been previously described (Nalbant et al., 2004). For each cell, eGFP and ISO-dye images were collected. Correlation analysis between the total expression of GFP and the ISO-GFP signal showed that the ratio decreased significantly with increased expression of the biosensor (supplementary material Fig. S2A). Based on that observation, all the cells analyzed were chosen from a pool of similar GFP expression, with total cell fluorescence being less than 700 arbitrary units (a.u.). The images were background-subtracted and corrected for registration. Both eGFP and ISO image were multiplied by a binary mask. Finally, the ISO image was divided by the GFP image. The mean ratio (ISO:eGFP) was maximal within the first 2 μm from the cell edge (supplementary material Fig. S2B). Cdc42 activity at the cell edge was quantified by defining a region of interest 2 μm inwards from the cell edge in the final (ratio) image. Image processing was performed using image J software (National Institutes of Health, MA).

Cell transfection with siRNA

Cdc42 siRNA has been previously described (Yamaguchi et al., 2005). SmartPool Cdc42 siRNA and K-Ras siRNA were obtained from Dharmacon. MTLn3 cells were transfected

with 100 nM Cdc42 siRNA or with control siRNA sequences targeting GL2 (Ambion) using Oligofectamine (Invitrogen) as described by the manufacturer. After 48 hours, protein levels in total cell lysates were analyzed by western blotting using antibodies against Cdc42.

Live upshift and motility assay

For motility analysis, images of cells in serum were collected every 60 seconds for 2 hours using a 20× objective, and their rate of movement was quantified using Image J and DIAS computational software (Wessels et al., 1998). Live imaging of cells in serum, which had been transfected with GFP-vinculin was performed every 30 seconds for 10 minutes. Optimal temperature and CO_2 control were maintained using an inverted Olympus IX70 microscope mounted in an incubation chamber. Kymographic analysis was performed on MTLn3 cells undergoing upshift and imaged every 20 seconds up to 10 minutes using a 60× objective. The time-lapse images were then stacked into time series using image J software, a line (1 μm) was drawn across the cell edge and then the expansion of the cell membrane along the line was projected in 2D as a function of time.

EGF receptor endocytosis

MTLn3 cells were plated in 24-well plates and transfected with luciferase or Cdc42 siRNA. After 48 hours, cells were starved for 3 hours at 37°C and then stimulated with ^{125}I-EGF. At the appropriate times, cells were placed on ice, rinsed six times with cold PBS, and surface-bound ^{125}I-EGF was released by ice-cold 0.2 M acetic acid containing 0.5 M NaCl (Wiley and Cunningham, 1982). Intracellular radioactivity was assessed by dissolving the acetic-acid-rinsed cultures in 2.5 ml of 1 N NaOH for 2 hours at 37°C. Nonspecific binding was measured in the presence of unlabeled EGF at 100 times excess, and was less than 2% of total binding. The value of the endocytic rate constant (k_e) was obtained by plotting internalized ligand against the integral over time of surface-associated ligand (Lund et al., 1990). Correlation coefficients of internalization plots were generally >0.9.

Electron microscopy

MTLn3 cells were grown on 5-mm glass coverslips, starved and stimulated with EGF for 3 minutes. The cells were then permeabilized and processed for rapid freeze-freeze dry-rotary shadow as previously described (Bailly et al., 1999). Coverslips were mounted on a rapid freezing apparatus (CF100; Life Cell Corp.) and frozen by slamming them into a liquid-nitrogen-cooled copper block. Samples were transferred to the specimen mount of a freeze-fracture apparatus (CFE-50; Cressington) and rotary-shadowed at a 45° angle with 1.2–1.3 nm tantalum-tungsten, and 2.5 nm carbon at 90°. The replicas were separated from the glass coverslips with 25% hydrofluoric acid, washed into distilled water and picked up onto the surface of Formvar-coated copper grids. The samples were examined by a JEOL 100CX transmission electron microscope at 100 kV and then the filament lengths and the incidence angle at the membrane were measured as previously described in details (Bailly et al., 1999; DesMarais et al., 2004).

Statistics

All error estimates are given as ± s.e.m.

Supplementary Material

Refer to Web version on PubMed Central for supplementary material.

Acknowledgments

The authors thank the Analytical Imaging Facility at Albert Einstein College of Medicine for technical help with image analysis. We would also thank Stefan Huettelmaier for providing the GFP-vinculin, and Jeff Segall (AECOM, New York, NY), Louis Hodgson (University of North Carolina, Chapel Hill) and Mark Symons (Northshore-Long Island Jewish, NY) for valuable discussions. This work was supported by National Institutes of Health grants CA 100324, GM057464 and GM064346.

References

Allen WE, Zicha D, Ridley AJ, Jones GE. A role for Cdc42 in macrophage chemotaxis. J Cell Biol. 1998; 141:1147–1157. [PubMed: 9606207]

Andrew N, Insall RH. Chemotaxis in shallow gradients is mediated independently of PtdIns 3-kinase by biased choices between random protrusions. Nat Cell Biol. 2007; 9:193–200. [PubMed: 17220879]

Bailly M, Macaluso F, Cammer M, Chan A, Segall JE, Condeelis JS. Relationship between Arp2/3 complex and the barbed ends of actin filaments at the leading edge of carcinoma cells after epidermal growth factor stimulation. J Cell Biol. 1999; 145:331–345. [PubMed: 10209028]

Bailly M, Ichetovkin I, Grant W, Zebda N, Machesky LM, Segall JE, Condeelis J. The F-actin side binding activity of the Arp2/3 complex is essential for actin nucleation and lamellipod extension. Curr Biol. 2001; 11:620–625. [PubMed: 11369208]

Benard V, Bokoch GM. Assay of Cdc42, Rac, and Rho GTPase activation by affinity methods. Meth Enzymol. 2002; 345:349–359. [PubMed: 11665618]

Chan AY, Raft S, Bailly M, Wyckoff JB, Segall JE, Condeelis JS. EGF stimulates an increase in actin nucleation and filament number at the leading edge of the lamellipod in mammary adenocarcinoma cells. J Cell Sci. 1998; 111:199–211. [PubMed: 9405304]

Chan AY, Bailly M, Zebda N, Segall JE, Condeelis JS. Role of cofilin in epidermal growth factor-stimulated actin polymerization and lamellipod protrusion. J Cell Biol. 2000; 148:531–542. [PubMed: 10662778]

Chattopadhyay A, Vecchi M, Ji Q, Mernaugh R, Carpenter G. The role of individual SH2 domains in mediating association of phospholipase C-gamma1 with the activated EGF receptor. J Biol Chem. 1999; 274:26091–26097. [PubMed: 10473558]

Chen L, Janetopoulos C, Huang YE, Iijima M, Borleis J, Devreotes PN. Two phases of actin polymerization display different dependencies on PI(3,4,5)P3 accumulation and have unique roles during chemotaxis. Mol Biol Cell. 2003; 14:5028–5037. [PubMed: 14595116]

Chou J, Burke NA, Iwabu A, Watkins SC, Wells A. Directional motility induced by epidermal growth factor requires Cdc42. Exp Cell Res. 2003; 287:47–56. [PubMed: 12799181]

Cox D, Chang P, Zhang Q, Reddy PG, Bokoch GM, Greenberg S. Requirements for both Rac1 and Cdc42 in membrane ruffling and phagocytosis in leukocytes. J Exp Med. 1997; 186:1487–1494. [PubMed: 9348306]

DesMarais V, Ichetovkin I, Condeelis J, Hitchcock-DeGregori SE. Spatial regulation of actin dynamics: a tropomyosin-free, actin-rich compartment at the leading edge. J Cell Sci. 2002; 115:4649–4660. [PubMed: 12415009]

DesMarais V, Macaluso F, Condeelis J, Bailly M. Synergistic interaction between the Arp2/3 complex and cofilin drives stimulated lamellipod extension. J Cell Sci. 2004; 117:3499–3510. [PubMed: 15252126]

Eddy RJ, Pierini LM, Matsumura F, Maxfield FR. Ca2+-dependent myosin II activation is required for uropod retraction during neutrophil migration. J Cell Sci. 2000; 113:1287–1298. [PubMed: 10704379]

Eden S, Rohatgi R, Podtelejnikov AV, Mann M, Kirschner MW. Mechanism of regulation of WAVE1-induced actin nucleation by Rac1 and Nck. Nature. 2002; 418:790–793. [PubMed: 12181570]

Ferguson GJ, Milne L, Kulkarni S, Sasaki T, Walker S, Andrews S, Crabbe T, Finan P, Jones G, Jackson S, et al. PI(3)Kgamma has an important context-dependent role in neutrophil chemokinesis. Nat Cell Biol. 2007; 9:86–91. [PubMed: 17173040]

Funamoto S, Meili R, Lee S, Parry L, Firtel RA. Spatial and temporal regulation of 3-phosphoinositides by PI 3-kinase and PTEN mediates chemotaxis. Cell. 2002; 109:611–623. [PubMed: 12062104]

Gardiner EM, Pestonjamasp KN, Bohl BP, Chamberlain C, Hahn KM, Bokoch GM. Spatial and temporal analysis of Rac activation during live neutrophil chemotaxis. Curr Biol. 2002; 12:2029–2034. [PubMed: 12477392]

Hall A. Rho GTPases and the actin cytoskeleton. Science. 1998; 279:509–514. [PubMed: 9438836]

Hall AL, Warren V, Dharmawardhane S, Condeelis J. Identification of actin nucleation activity and polymerization inhibitor in ameboid cells: their regulation by chemotactic stimulation. J Cell Biol. 1989; 109:2207–2213. [PubMed: 2553744]

Han J, Luby-Phelps K, Das B, Shu X, Xia Y, Mosteller RD, Krishna UM, Falck JR, White MA, Broek D. Role of substrates and products of PI 3-kinase in regulating activation of Rac-related guanosine triphosphatases by Vav. Science. 1998; 279:558–560. [PubMed: 9438848]

Hawkins PT, Eguinoa A, Qiu RG, Stokoe D, Cooke FT, Walters R, Wennstrom S, Claesson-Welsh L, Evans T, Symons M, et al. PDGF stimulates an increase in GTP-Rac via activation of phosphoinositide 3-kinase. Curr Biol. 1995; 5:393–403. [PubMed: 7627555]

Hill K, Welti S, Yu J, Murray JT, Yip SC, Condeelis JS, Segall JE, Backer JM. Specific requirement for the p85-p110alpha phosphatidylinositol 3-kinase during epidermal growth factor-stimulated actin nucleation in breast cancer cells. J Biol Chem. 2000; 275:3741–3744. [PubMed: 10660520]

Hoeller O, Kay RR. Chemotaxis in the absence of PIP3 gradients. Curr Biol. 2007; 17:813–817. [PubMed: 17462897]

Hong-Geller E, Cerione RA. Cdc42 and Rac stimulate exocytosis of secretory granules by activating the IP(3)/calcium pathway in RBL-2H3 mast cells. J Cell Biol. 2000; 148:481–494. [PubMed: 10662774]

Huang YE, Iijima M, Parent CA, Funamoto S, Firtel RA, Devreotes P. Receptor-mediated regulation of PI3Ks confines PI(3,4,5)P3 to the leading edge of chemotaxing cells. Mol Biol Cell. 2003; 14:1913–1922. [PubMed: 12802064]

Ichetovkin I, Han J, Pang KM, Knecht DA, Condeelis JS. Actin filaments are severed by both native and recombinant dictyostelium cofilin but to different extents. Cell Motil Cytoskeleton. 2000; 45:293–306. [PubMed: 10744862]

Innocenti M, Zucconi A, Disanza A, Frittoli E, Areces LB, Steffen A, Stradal TE, Di Fiore PP, Carlier MF, Scita G. Abi1 is essential for the formation and activation of a WAVE2 signalling complex. Nat Cell Biol. 2004; 6:319–327. [PubMed: 15048123]

Krugmann S, Jordens I, Gevaert K, Driessens M, Vandekerckhove J, Hall A. Cdc42 induces filopodia by promoting the formation of an IRSp53:Mena complex. Curr Biol. 2001; 11:1645–1655. [PubMed: 11696321]

Kurokawa K, Nakamura T, Aoki K, Matsuda M. Mechanism and role of localized activation of Rho-family GTPases in growth factor-stimulated fibroblasts and neuronal cells. Biochem Soc Trans. 2005; 33:631–634. [PubMed: 16042560]

Lund KA, Opresko LK, StarBuck C, Walsh BJ, Wiley HS. Quantitative analysis of the endocytic system involved in hormone-induced receptor internalization. J Biol Chem. 1990; 265:15713–15723. [PubMed: 1975591]

Matsui S, Adachi R, Kusui K, Yamaguchi T, Kasahara T, Hayakawa T, Suzuki K. U73122 inhibits the dephosphorylation and translocation of cofilin in activated macrophage-like U937 cells. Cell Signal. 2001; 13:17–22. [PubMed: 11257443]

Miki H, Sasaki T, Takai Y, Takenawa T. Induction of filopodium formation by a WASP-related actin-depolymerizing protein N-WASP. Nature. 1998; 391:93–96. [PubMed: 9422512]

Miki H, Yamaguchi H, Suetsugu S, Takenawa T. IRSp53 is an essential intermediate between Rac and WAVE in the regulation of membrane ruffling. Nature. 2000; 408:732–735. [PubMed: 11130076]

Mouneimne G, Soon L, DesMarais V, Sidani M, Song X, Yip SC, Ghosh M, Eddy R, Backer JM, Condeelis J. Phospholipase C and cofilin are required for carcinoma cell directionality in response to EGF stimulation. J Cell Biol. 2004; 166:697–708. [PubMed: 15337778]

Mouneimne G, DesMarais V, Sidani M, Scemes E, Wang W, Song X, Eddy R, Condeelis J. Spatial and temporal control of cofilin activity is required for directional sensing during chemotaxis. Curr Biol. 2006; 16:2193–2205. [PubMed: 17113383]

Nakahara H, Otani T, Sasaki T, Miura Y, Takai Y, Kogo M. Involvement of Cdc42 and Rac small G proteins in invadopodia formation of RPMI7951 cells. Genes Cells. 2003; 8:1019–1027. [PubMed: 14750956]

Nalbant P, Hodgson L, Kraynov V, Toutchkine A, Hahn KM. Activation of endogenous Cdc42 visualized in living cells. Science. 2004; 305:1615–1619. [PubMed: 15361624]

Nishio M, Watanabe K, Sasaki J, Taya C, Takasuga S, Iizuka R, Balla T, Yamazaki M, Watanabe H, Itoh R, et al. Control of cell polarity and motility by the PtdIns(3,4,5)P3 phosphatase SHIP1. Nat Cell Biol. 2007; 9:36–44. [PubMed: 17173042]

Nobes CD, Hall A. Rho, rac, and cdc42 GTPases regulate the assembly of multimolecular focal complexes associated with actin stress fibers, lamellipodia, and filopodia. Cell. 1995; 81:53–62. [PubMed: 7536630]

O'Connor KL, Nguyen BK, Mercurio AM. RhoA function in lamellae formation and migration is regulated by the alpha6beta4 integrin and cAMP metabolism. J Cell Biol. 2000; 148:253–258. [PubMed: 10648558]

Oikawa T, Yamaguchi H, Itoh T, Kato M, Ijuin T, Yamazaki D, Suetsugu S, Takenawa T. PtdIns(3,4,5)P3 binding is necessary for WAVE2-induced formation of lamellipodia. Nat Cell Biol. 2004; 6:420–426. [PubMed: 15107862]

Olson MF, Pasteris NG, Gorski JL, Hall A. Faciogenital dysplasia protein (FGD1) and Vav, two related proteins required for normal embryonic development, are upstream regulators of Rho GTPases. Curr Biol. 1996; 6:1628–1633. [PubMed: 8994827]

Pertz O, Hahn KM. Designing biosensors for Rho family proteins – deciphering the dynamics of Rho family GTPase activation in living cells. J Cell Sci. 2004; 117:1313–1318. [PubMed: 15020671]

Pollard TD, Borisy GG. Cellular motility driven by assembly and disassembly of actin filaments. Cell. 2003; 112:453–465. [PubMed: 12600310]

Ponti A, Machacek M, Gupton SL, Waterman-Storer CM, Danuser G. Two distinct actin networks drive the protrusion of migrating cells. Science. 2004; 305:1782–1786. [PubMed: 15375270]

Ridley AJ. Rho family proteins: coordinating cell responses. Trends Cell Biol. 2001; 11:471–477. [PubMed: 11719051]

Rohatgi R, Ma L, Miki H, Lopez M, Kirchhausen T, Takenawa T, Kirschner MW. The interaction between N-WASP and the Arp2/3 complex links Cdc42-dependent signals to actin assembly. Cell. 1999; 97:221–231. [PubMed: 10219243]

Rotsch C, Jacobson K, Condeelis J, Radmacher M. EGF-stimulated lamellipod extension in adenocarcinoma cells. Ultramicroscopy. 2001; 86:97–106. [PubMed: 11215638]

Schlessinger J. How receptor tyrosine kinases activate Ras. Trends Biochem Sci. 1993; 18:273–275. [PubMed: 8236435]

Segall JE, Tyerech S, Boselli L, Masseling S, Helft J, Chan A, Jones J, Condeelis J. EGF stimulates lamellipod extension in metastatic mammary adenocarcinoma cells by an actin-dependent mechanism. Clin Exp Metastasis. 1996; 14:61–72. [PubMed: 8521618]

Soderling SH, Scott JD. WAVE signalling: from biochemistry to biology. Biochem Soc Trans. 2006; 34:73–76. [PubMed: 16417486]

Stradal TE, Scita G. Protein complexes regulating Arp2/3-mediated actin assembly. Curr Opin Cell Biol. 2006; 18:4–10. [PubMed: 16343889]

Suetsugu S, Kurisu S, Oikawa T, Yamazaki D, Oda A, Takenawa T. Optimization of WAVE2 complex-induced actin polymerization by membrane-bound IRSp53, PIP(3), and Rac. J Cell Biol. 2006; 173:571–585. [PubMed: 16702231]

Toutchkine A, Kraynov V, Hahn K. Solvent-sensitive dyes to report protein conformational changes in living cells. J Am Chem Soc. 2003; 125:4132–4145. [PubMed: 12670235]

Vanhaesebroeck B, Jones GE, Allen WE, Zicha D, Hooshmand-Rad R, Sawyer C, Wells C, Waterfield MD, Ridley AJ. Distinct PI(3)Ks mediate mitogenic signalling and cell migration in macrophages. Nat Cell Biol. 1999; 1:69–71. [PubMed: 10559867]

Weiner OD, Neilsen PO, Prestwich GD, Kirschner MW, Cantley LC, Bourne HR. A PtdInsP(3)- and Rho GTPase-mediated positive feedback loop regulates neutrophil polarity. Nat Cell Biol. 2002; 4:509–513. [PubMed: 12080346]

Wessels D, Voss E, Von Bergen N, Burns R, Stites J, Soll DR. A computer-assisted system for reconstructing and interpreting the dynamic three-dimensional relationships of the outer surface, nucleus and pseudopods of crawling cells. Cell Motil Cytoskeleton. 1998; 41:225–246. [PubMed: 9829777]

Wheeler AP, Wells CM, Smith SD, Vega FM, Henderson RB, Tybulewicz VL, Ridley AJ. Rac1 and Rac2 regulate macrophage morphology but are not essential for migration. J Cell Sci. 2006; 119:2749–2757. [PubMed: 16772332]

Wiley HS, Cunningham DD. The endocytic rate constant: a cellular parameter for quantitating receptor-mediated endocytosis. J Biol Chem. 1982; 257:4222–4229. [PubMed: 6279628]

Yamaguchi H, Condeelis J. Regulation of the actin cytoskeleton in cancer cell migration and invasion. Biochim Biophys Acta. 2007; 1773:642–652. [PubMed: 16926057]

Yamaguchi H, Lorenz M, Kempiak S, Sarmiento C, Coniglio S, Symons M, Segall J, Eddy R, Miki H, Takenawa T, et al. Molecular mechanisms of invadopodium formation: the role of the N-WASP-Arp2/3 complex pathway and cofilin. J Cell Biol. 2005; 168:441–452. [PubMed: 15684033]

Yip S, El-Sibai M, Coniglio SJ, Mouneimne G, Eddy RJ, Drees BE, Neilsen PO, Goswami S, Symons M, Condeelis JS, Backer J. The distinct roles of Ras and Rac in PI 3-kinase dependent protrusion during EGF-stimulated cell migration. J Cell Sci. 2007; 120:3138–3146. [PubMed: 17698922]

Yonezawa N, Nishida E, Iida K, Yahara I, Sakai H. Inhibition of the interactions of cofilin, destrin, and deoxyribonuclease I with actin by phosphoinositides. J Biol Chem. 1990; 265:8382–8386. [PubMed: 2160454]

Zheng Y, Bagrodia S, Cerione RA. Activation of phosphoinositide 3-kinase activity by Cdc42Hs binding to p85. J Biol Chem. 1994; 269:18727–18730. [PubMed: 8034624]

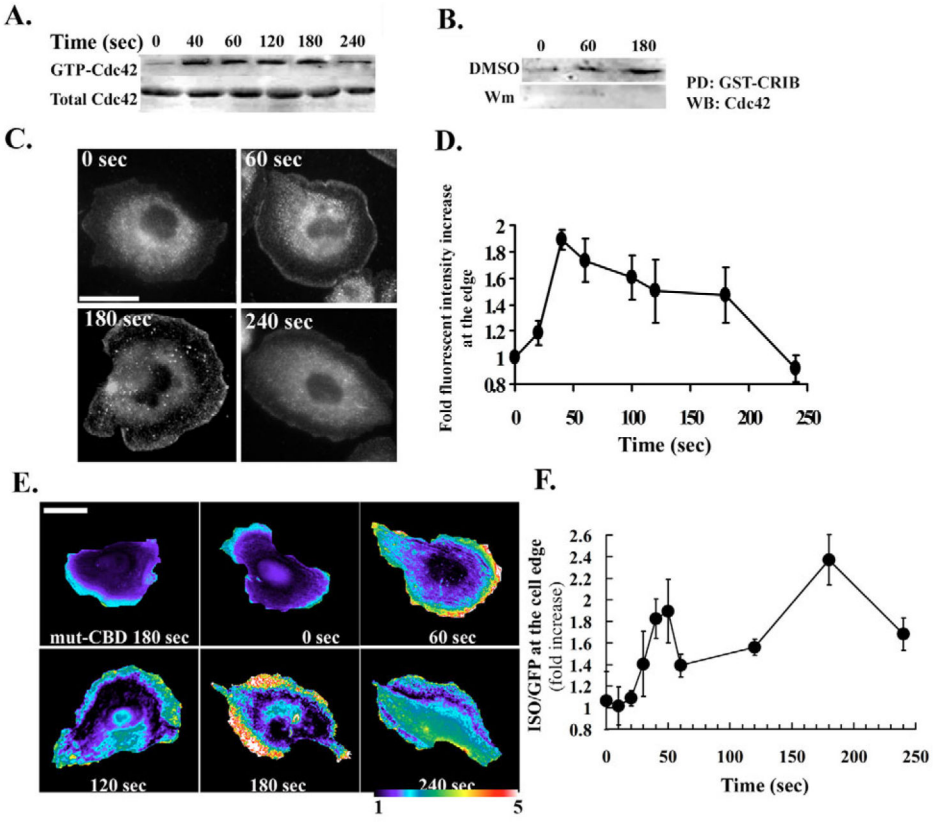

Fig. 1.

Cdc42 activation at the protruding edge in response to EGF stimulation. MTLn3 cells were serum-starved for 3 hours and then stimulated with 5 nM EGF at 37°C for the indicated times. (A) GST-CRIB pull-downs of unstimulated and stimulated cells. Anti-Cdc42 western blots showing activated (GTP-Cdc42) and total Cdc42. The data are representative of three experiments. (B) GST-CRIB assay for Cdc42 activation in cells pre-treated with carrier (DMSO) or 100 nM wortmannin (Wm) for 15 minutes, then stimulated with EGF. (C) Representative micrographs of EGF-stimulated cells, fixed at various times and immunostained with anti-Cdc42 antibody. (D) Quantification of data shown in C; fluorescence intensity in the lamellipod edge (0.2–0.6 μm in from the edge of the cell) was normalized to edge intensity of non-stimulated cells. The data is the mean ±s.e.m. from three different experiments (15 cells per experiment), plotted as a function of time. (E) MTLn3 cells were starved for 3 hours and microinjected with the Cdc42 biosensor as explained in Materials and Methods. After 1 hour, cells were stimulated with 5 nM EGF for various times, or not (0 minutes), and fixed. Ratio images (I-SO:GFP) reflect the activation (GTP binding) of Cdc42 at different times after EGF stimulation. Activation was maximal at the 180 seconds, with regions of highest activity five times greater than in the unstimulated cells. (F) At each time point, the mean ratio from a region of interest (2 μm inwards from the edge to the center of the cell) is calculated as fold increase relative to unstimulated cells, and plotted as a function of time. Data are the mean ± s.e.m. from 40 different cells. Bars, 10 μm.

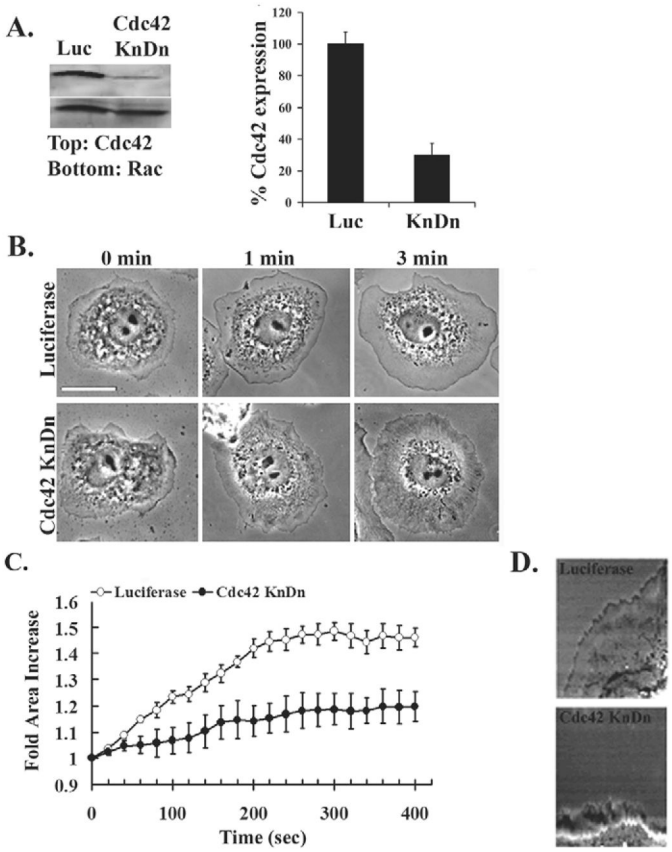

Fig. 2.

Cdc42-siRNA-treated cells show reduced protrusion in response to EGF stimulation. (A) Representative western blot showing Cdc42 (upper panel) and Rac (lower panel) expression in cells treated with control luciferase-siRNA-treated (Luc) or Cdc42 siRNA (Cdc42 KnDn). Quantification of western blots from four different experiments (bar graph) shows an 80% decrease in the level of expression of Cdc42 in cell lysates. (B) Representative phase micrographs of MTLn3 cells transfected with control luciferase or Cdc42 siRNA (Cdc42 KnDn), starved and stimulated with EGF for 1 or 3 minutes or not (0 min). (C) Quantification of the surface area of EGF-stimulated control luciferase-siRNA-treated (○) and Cdc42-siRNA-treated cells (●) normalized to unstimulated cells. Data are the mean ± s.e.m. from at least 45 cells. Bar, 10 μm. (D) MTLn3 cells were transfected with luciferase control or Cdc42 siRNA and starved for 3 hours. Cells were then imaged using time-lapse microscopy during a 10-minute EGF stimulation with images collected every 20 seconds. Kymographs were generated by drawing a constant line in the stacked time series and the protrusion was followed over time.

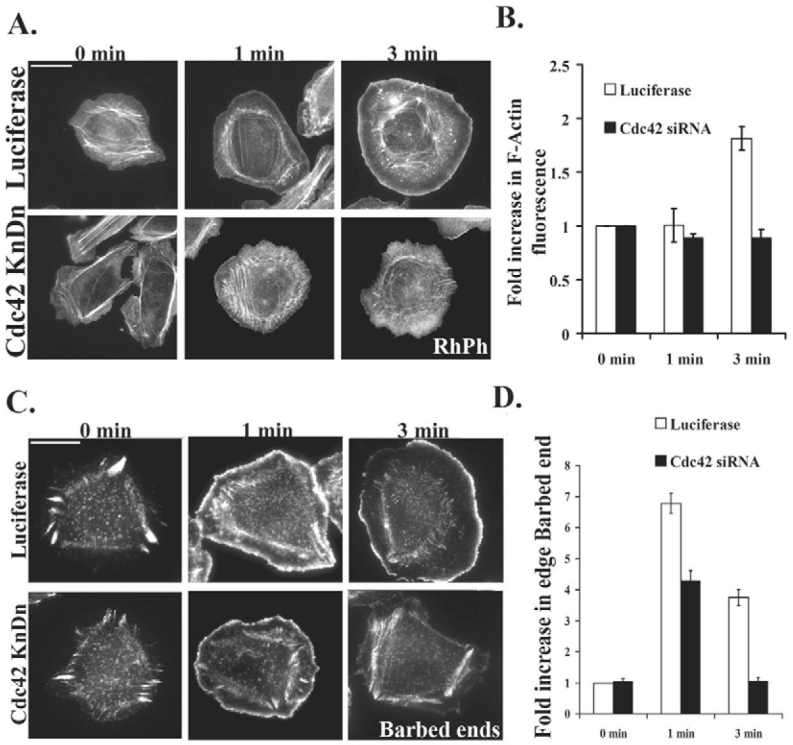

Fig. 3.

Cdc42-siRNA-treated cells show a loss of actin nucleation at the protruding edge in response to EGF stimulation. (A) Representative micrographs of MTLn3 cells transfected with control luciferase or Cdc42 siRNA, starved for 3 hours and stimulated with EGF for 1 or 3 minutes or not (0 min). Cells are stained with Rhodamine-phalloidin to visualize F-actin. (B) Quantification of the average F-actin fluorescence at the protruding edge (0.2–0.6 μm in from the edge of the cell) normalized to edge intensity of non-stimulated cells. Data are the mean ± s.e.m. from three different experiments (15 cells per experiment). (C) Control and Cdc42 siRNA-treated MTLn3 cells were stimulated with EGF for 1 or 3 minutes or not (0 min), permeabilized and incubated with biotin-actin, and immunostained with anti-biotin to detect the newly formed barbed ends. (D) Quantification of barbed-end formation at the protruding edge (0.2–0.6 μm in from the periphery) normalized to unstimulated cells. Data are the mean fluorescence ± s.e.m. from three different experiments (15 cells per experiment). Bars, 10 μm.

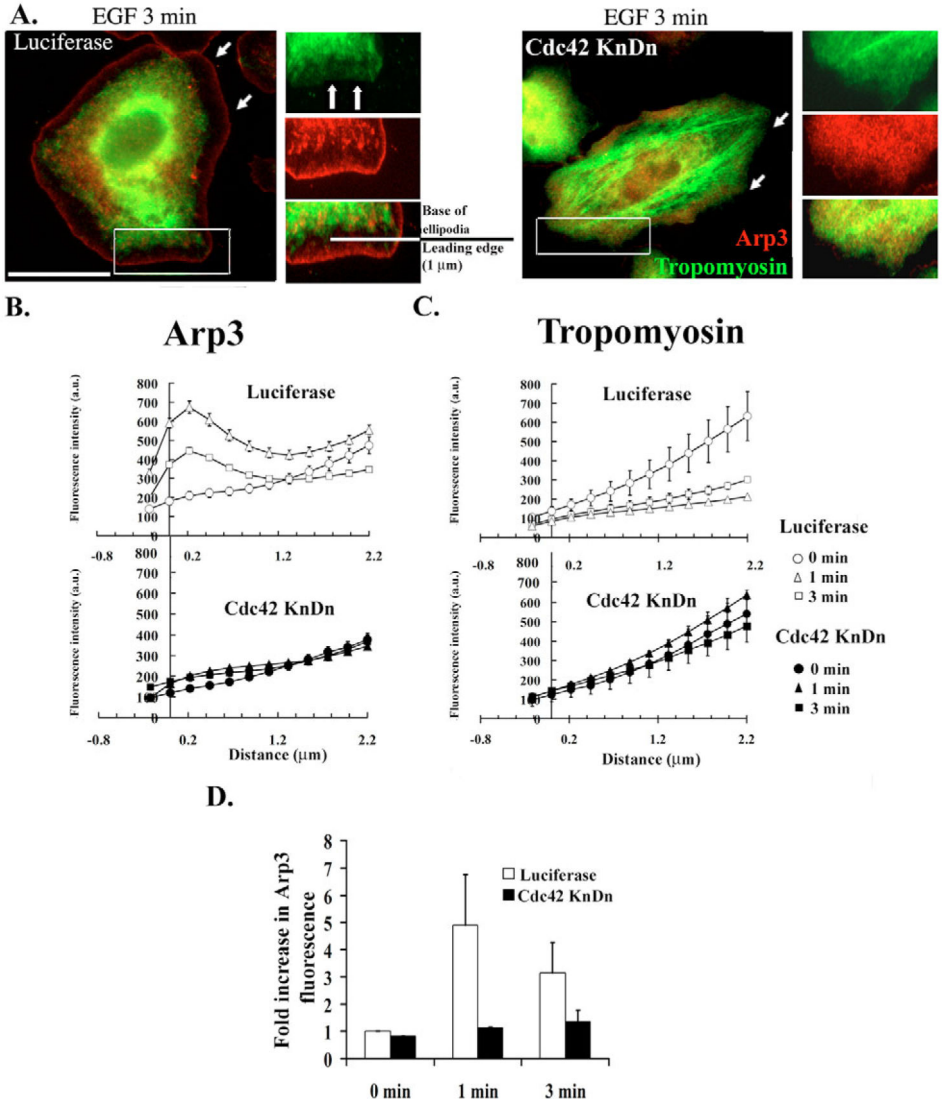

Fig. 4.

Cdc42 meditates the translocation of Arp2/3 to the protruding edge in response to EGF stimulation. MTLn3 cells were transfected with control or Cdc42 siRNA, starved for 3 hours and stimulated with EGF for 1 or 3 minutes or not. The cells were then fixed and immunostained with anti-Arp3 and anti-tropomyosin antibodies. (A) Representative merged images of control luciferase-siRNA-treated (left panels) or Cdc42-siRNA-treated (right panels) cells stimulated for 3 minutes and stained for Arp3 (red) and Tropomyosin (green). Small panels show magnification of boxed areas of respective large panel. Arrows indicate the edges of Arp2/3 (red) and tropomyosin-rich (green) zones. (B) Quantification of average fluorescence pixel intensity at the edge for Arp2/3 in control luciferase-siRNA-treated (top diagram) and Cdc42-siRNA-treated (bottom diagram) cells stimulated with EGF for 1 minute (△ and ▲, respectively) or 3 minutes (□ and ■, respectively) or left untreated (○ and ●, respectively). Data are the mean ± s.e.m. from three different experiments (15 cells per experiment) plotted as a function of distance from the cell edge. (C) Quantification of

average fluorescence pixel intensity at the edge for tropomyosin in control (top diagram) and Cdc42 siRNA-treated cells (top diagram). Cells were stimulated as in B. (D) Data from B presented as an average of the mean fluorescence in the lamellipodia (0.2–0.6 μm from the edge) normalized to unstimulated cells. Bar, 10 μm.

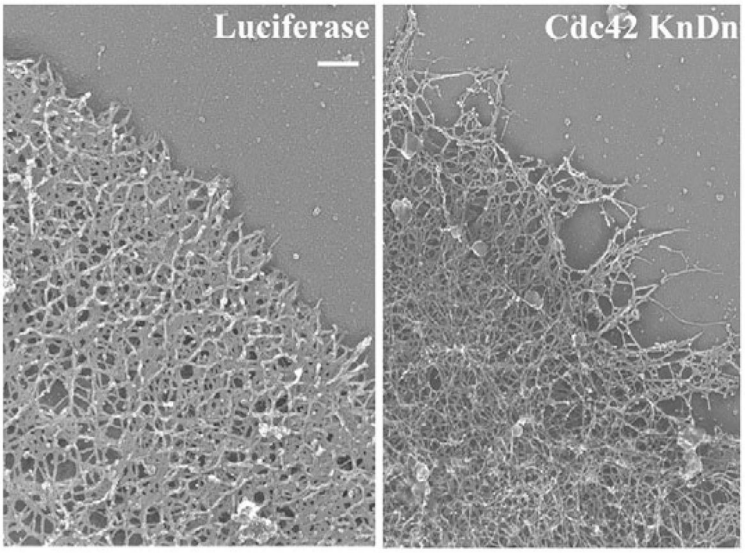

Fig. 5.

Cdc42 is required for actin branching at the protruding edge. Rotary-shadowing transmission electron micrographs of cells treated with control luciferase (left panel) or Cdc42 (right panel) siRNA (*n*=10 cells). Bar, 100 nm.

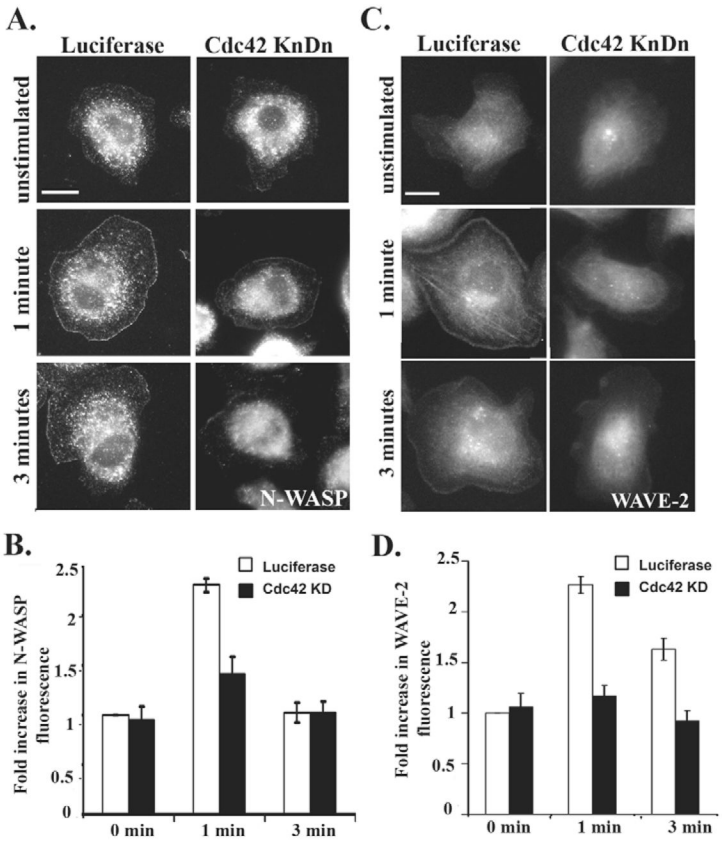

Fig. 6.

Cdc42 mediates the translocation of N-WASP and WAVE2 to the edge in response to EGF. Control luciferase-siRNA-transfected or Cdc42-siRNA-transfected (Cdc42 KnDn) MTLn3 cells were starved for 3 hours, and stimulated with EGF for 1 or 3 minutes, or not. (A) Representative images of cells immunostained with anti-N-WASP antibody. (B) The average N-WASP fluorescence in the lamellipodia (0.2–0.6 μm in from the edge) was measured as explained in Materials and Methods and normalized to edge fluorescence of unstimulated cells. (C) Representative images of cells immunostained with anti-WAVE2 antibody. (D) The average WAVE2 fluorescence in the lamellipodia (0.2–0.6 μm in from the edge) was measured as explained in Materials and Methods and normalized to edge fluorescence of unstimulated cells. Data in B and D are the mean ± s.e.m. from 45 cells for each staining condition. Bars, 10 μm.

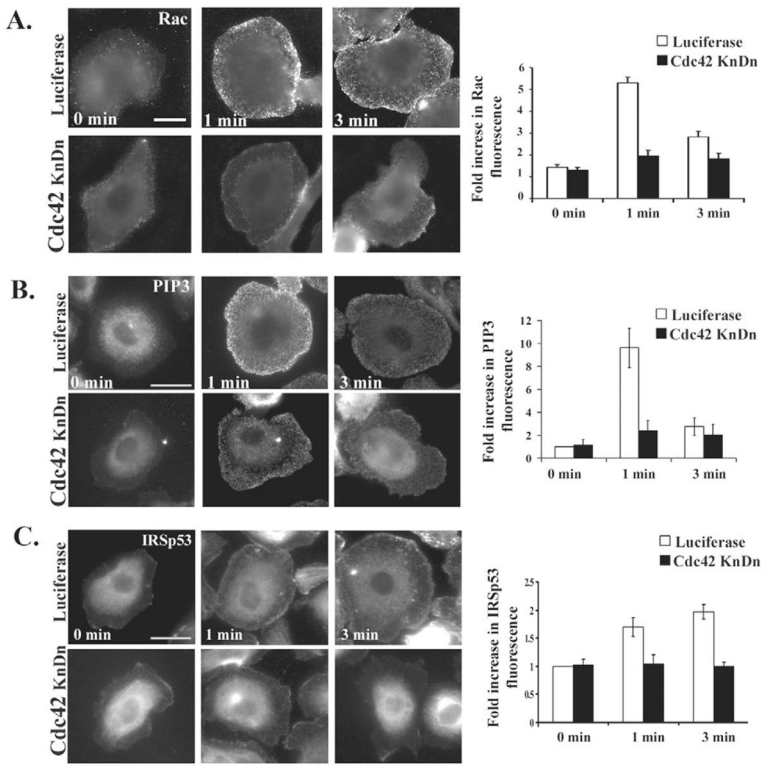

Fig. 7.

Cdc42 is required for activation of Rac, PI3K and IRSp53 at the protruding edge of EGF-stimulated cells. Control luciferase-siRNA-transfected or Cdc42-siRNA-transfected MTLn3 cells were starved for 3 hours, and stimulated with EGF for 1 or 3 minutes, or not. Representative images of cells immunostained against (A) Rac, (B) PtdIns(3,4,5)P_3 or (C) IRSp53. Bar graphs show the average Rac, PtdIns(3,4,5)P_3 or IRSp53 fluorescence in the lamellipodia (0.2–0.6 μm from the edge), normalized to edge fluorescence of unstimulated cells. Data are the mean ± s.e.m. from 45 cells. Bars, 10 μm.

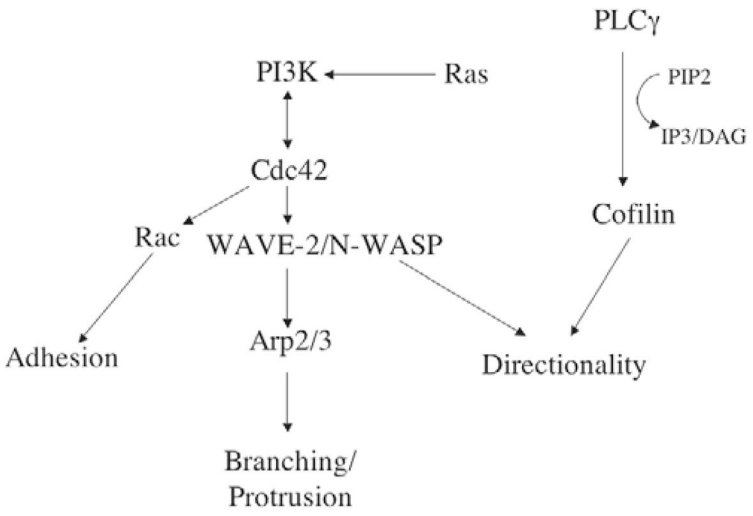

Fig. 8.

Model of Cdc42-mediated cytoskeletal signaling in carcinoma cells. Cdc42 and PI3K are both activated within the first minute of EGF stimulation in carcinoma cells, and might form a positive feedback loop. At later times, PI3K also receives input from Ras, which is required for protrusion. Activated Cdc42 is upstream of Rac, which regulates the formation of adhesive structures behind the protruding edge. Cdc42 regulation of WAVE2 and/or N-WASP is required for recruitment and activation of Arp2/3 and formation of branching actin structures. Cdc42 activation of N-WASP might also be involved in directional sensing (Nakahara et al., 2003; Yamaguchi et al., 2005), in tandem with PLCγ-mediated activation of cofilin (Mouneimne et al., 2004).

Table 1

Cdc42 knockdown reduces the motility of carcinoma cells

	Total path (μm)	Net path (μm)
A		
Control oligomer (luciferase)	70.3±5.6	22.9±0.4
Cdc42 siRNA	37.5±3.6	16.9±0.5
B		
Control oligomer (luciferase)	60.2±1.2	23.0±1.8
Cdc42 siRNA pooled oligomers	34.5±2.4	10.2±1.4

A, MTLn3 cells were transfected with luciferase control siRNA (Movie 1) or with Cdc42 siRNA (Movie 2); *n*=50 cells, data are mean ± s.e.m. B, MTLn3 cells were transfected with luciferase siRNA or with SmartPool Cdc42 siRNA (30 cells). The cells were imaged in medium containing 5% FBS for 2 hours. The time interval between successive frames was 1 minute. Mobility parameters were calculated with DIAS software (Wessels et al., 1998). Differences in all presented parameters are statistically significant; *n*=50 cells.